INFECTION AND IMMUNITY, Oct. 2002, p. 5730–5739 Vol. 70, No. 10
0019-9567/02/$04.00+0 DOI: 10.1128/IAI.70.10.5730–5739.2002

Identification of a Streptolysin S-Associated Gene Cluster and Its Role in the Pathogenesis of *Streptococcus iniae* Disease

Jeffrey D. Fuller,[1,2] Alvin C. Camus,[3] Carla L. Duncan,[2] Victor Nizet,[4] Darrin J. Bast,[1,2] Ronald L. Thune,[3] Donald E. Low,[1,2] and Joyce C. S. de Azavedo[1,2]*

Department of Laboratory Medicine and Pathobiology, University of Toronto,[1] and Department of Microbiology, Mount Sinai Hospital, and Toronto Medical Laboratories, University Health Network,[2] Toronto, Ontario, Canada; Department of Pathological Sciences, School of Veterinary Medicine, Louisiana State University, Baton Rouge, Louisiana[3]; and Division of Pediatric Infectious Diseases, University of California, San Diego School of Medicine, La Jolla, California[4]

Received 30 January 2002/Returned for modification 26 March 2002/Accepted 27 June 2002

Streptococcus iniae **causes meningoencephalitis and death in cultured fish species and soft-tissue infection in humans. We recently reported that *S. iniae* is responsible for local tissue necrosis and bacteremia in a murine subcutaneous infection model. The ability to cause bacteremia in this model is associated with a genetic profile unique to strains responsible for disease in fish and humans (J. D. Fuller, D. J. Bast, V. Nizet, D. E. Low, and J. C. S. de Azavedo, Infect. Immun. 69:1994-2000, 2001). *S. iniae* produces a cytolysin that confers a hemolytic phenotype on blood agar media. In this study, we characterized the genomic region responsible for *S. iniae* cytolysin production and assessed its contribution to virulence. Transposon (Tn*917*) mutant libraries of commensal and disease-associated *S. iniae* strains were generated and screened for loss of hemolytic activity. Analysis of two nonhemolytic mutants identified a chromosomal locus comprising 9 genes with 73% homology to the group A streptococcus (GAS) *sag* operon for streptolysin S (SLS) biosynthesis. Confirmation that the *S. iniae* cytolysin is a functional homologue of SLS was achieved by PCR ligation mutagenesis, complementation of an SLS-negative GAS mutant, and use of the SLS inhibitor trypan blue. SLS-negative *sagB* mutants were compared to their wild-type *S. iniae* parent strains in the murine model and in human whole-blood killing assays. These studies demonstrated that *S. iniae* SLS expression is required for local tissue necrosis but does not contribute to the establishment of bacteremia or to resistance to phagocytic clearance.**

Streptococcus iniae is a hemolytic, gram-positive coccus that causes meningoencephalitis and significant mortality in a variety of commercial fish species, creating a substantial economic burden for the aquaculture industry (12, 13, 41, 42). *S. iniae* also causes fulminant soft-tissue infection in humans, with associated bacteremia, following percutaneous injury acquired while handling whole fish (48). Although our understanding of the pathogenicity of this organism is poor, pulsed-field gel electrophoresis (PFGE) has revealed that strains causing disease in fish and strains causing disease in humans are clonally related, whereas commensal isolates from nondiseased fish are genetically diverse (48). We recently reported that this unique genetic profile was associated with virulence in experimental model systems. Disease-associated strains caused significant weight loss and bacteremia in a murine model of subcutaneous infection, exhibited resistance to phagocytic clearance in human whole blood, and were cytotoxic to human endothelial cells in vitro (19). From these findings we hypothesized that this unique genetic profile indicated the presence of one or more virulence determinants important to disease.

One of the few distinguishing phenotypes of *S. iniae* is the zone of beta-hemolysis surrounding colonies cultured on blood agar (42). Hemolysins, or cytolysins, are well-recognized features of many bacterial species, including streptococci, and are generally associated with damage to the membranes of a variety of mammalian cell types. Examples of streptococcal cytolysins include streptolysin O (SLO) and streptolysin S (SLS) of group A streptococci (GAS), the beta-hemolysin/cytolysin of group B streptococci (GBS), and the pneumolysin of *Streptococcus pneumoniae*, each of which has been implicated as a virulence factor in animal models of infection (3, 4, 33, 49). In this investigation, we describe a molecular approach used to identify the genetic locus responsible for cytolysin production in *S. iniae*. The contribution of the *S. iniae* cytolysin to disease pathogenesis was examined by using a murine model of subcutaneous infection.

MATERIALS AND METHODS

Bacterial strains, media, and transformation. Bacterial strains used in this study are listed in Table 1. *S. iniae* and other gram-positive bacterial strains were grown in Todd-Hewitt broth (THB) or on Columbia base agar (Difco, Detroit, Mich.) supplemented with 5% defibrinated sheep erythrocytes (SBA) (Quelab). Mid-log-phase cells were prepared from overnight cultures that were diluted 1/25 in THB and incubated at 37°C for 3 to 6 h. An optical density measurement of 0.35 to 0.40 at 620 nm, by use of a spectrophotometer (Beckman Instruments, Fullerton, Calif.), corresponded to mid-log-phase growth (10^8 CFU). For anaerobic conditions, cultures were incubated in anaerobic jars with an AnaeroGen pack (Oxoid). *Escherichia coli* was grown in Luria-Bertani (LB) broth or on LB agar (Difco). Antibiotics were used at the following concentrations: ampicillin, 100 μg/ml; erythromycin (ERY), 5 (for GAS) or 300 (for *E. coli* MC1061) μg/ml; chloramphenicol (CHL), 2 to 4 (for GAS) or 2.5 (for *S. iniae*) μg/ml. Gram-positive strains were rendered competent for transformation by growth in THB plus 0.6% glycine as described for GBS (18). *E. coli* MC1061 was rendered competent by standard methods (11), and *E. coli* TOP10 competent cells were obtained from Invitrogen Life Technologies. Plasmids were introduced by electroporation (at 1,500 V; Eppendorf model 2510) and immediately transferred

* Corresponding author. Mailing address: Department of Microbiology, Rm. 1483, Mount Sinai Hospital, 600 University Ave., Toronto, Ontario, Canada M5G 1X5. Phone: (416) 586-8459. Fax: (416) 586-8746. E-mail: jdeazavedo@mtsinai.on.ca.

TABLE 1. Bacterial strains and plasmids

Bacterial strain or plasmid	Description	Reference or source
Bacterial strains		
S. iniae		
9117	Disease-associated blood culture isolate from patient with cellulitis	19
9066	Commensal isolate from surface of healthy fish	19
9174	Commensal isolate from surface of healthy fish	This study
SI *sagB*.KO.*erm*	Nonhemolytic insertion/deletion mutant of 9117	This study
SI *sagB*.KO.Tn*917*	Nonhemolytic Tn*917* mutant of 9174	This study
GAS		
NZ131	T14/M49 clinical isolate from patient with glomerulonephritis; SLS^+	44
NZ131 *sagA*Δ*cat*	Nonhemolytic allelic replacement mutant of NZ131	Datta et al., Abstr. 6th Ann. Streptococcal Genetics Conf. abstr. 132
E. coli		
MC1061	F^- *araD139* Δ(*araABC-leu*)*7696* Δ*lacX74 galU galK hsdR2*(r_K^- m_K^+) *mcrB1 rpsL* (Str^r)	50
TOP10	F^- *mcA* Δ(*mrr-hsd* RMS-*mcrBC*) ϕ80 *dlacZ* ΔM15 Δ(*lacZ*)*X74 deoR recA1 araD139* Δ(*ara-leu*)*7697 galU galK rpsL* (Str^r)end *A1 nup G*	22
Plasmids		
pTV_1OK	*repA*(Ts)-pWV01(Ts) *aphA3* Tn*917* (*erm*)	23
pUC19	*lacZ*α *bla*	Pharmacia
pVE6007Δ	Temperature-sensitive derivative of pWV01; Cm^r	35
pCR2.1-TOPO	ColE *ori* Amp^r Km^r *lacZ*α	Invitrogen
pSI*sagB*.KO.*erm*	pVE6007Δ + 2,782-bp *ermB* allelic replacement construct	This study
pDC123	*E. coli*/streptococcal shuttle vector, JS-3 replicon; Cm^r	8
pSI*sagA*	pDC123 + 196-bp PCR amplicon of *S. iniae sagA*	This study

into 1 ml of recovery medium (for GAS, THB plus 0.25 M sucrose; for *E. coli*, SOC) for 1 to 3 h, at permissive temperatures, prior to antibiotic selection on agar media. Genomic and plasmid DNAs were extracted by previously described methods (5, 18, 46).

Primers and DNA sequencing. Oligonucleotide primers are listed in Table 2. DNA sequences were obtained by using an automated sequencer (ABI Prism; Applied Biosystems, Oakville, Ontario, Canada) at the Center for Applied Genomics, DNA Sequencing Facility, Hospital for Sick Children (Toronto, Ontario, Canada). The *S. iniae* sequence was compared with those in the GenBank databases by using the BLAST local alignment program of the National Center for Biotechnology Information, National Institutes of Health (1), and was aligned and annotated by using Vector NTI (InforMax, Inc.) software.

Tn*917* mutagenesis and identification of transposon insertion sites. Insertional mutagenesis of *S. iniae* strains 9117 and 9174 was performed as described for *Streptococcus mutans* by using the temperature-sensitive plasmid pTV_1OK, which harbors the conjugative transposon Tn*917* (23). Insertional libraries were screened on SBA for nonhemolytic (NH) transconjugants, and the genomic junction sites of Tn*917* insertions were identified as follows. The junction site containing the transposon-associated *ermB* gene in SINH3, derived from the disease-associated strain 9117, was cloned as a *Hin*dIII fragment in pUC19, transformed into *E. coli* MC1061, selected on ERY, and sequenced by using the *ermB* R and M13 universal primers. DNA from the insertion sites of the mutants SINH1, derived from the disease-associated strain 9117, and SI *sagB*.KO.Tn*917*, derived from the commensal strain 9174, was isolated by using a novel PCR-based method described by Karlyshev and colleagues (26). Transposon-specific, outward-reading primers ltp-1 and rtp-1 were used for the single-primer PCR amplification of up- and downstream *Tn*917-junction sites, respectively, from the genomic DNA template. Reactions utilized *Taq* DNA polymerase (Invitrogen Life Technologies) under the following cycling conditions: 2 min at 94°C; 20 cycles of 94°C for 30 s, 57°C for 30 s, and 72°C for 3 min; 30 cycles of 94°C for

TABLE 2. Primer list

Primer	Sequence	Description
ermB F	5′ TGCGTCTGACATCTATCTGATTG 3′	Tn*917* left, *ermB* intragenic primer
ermB R	5′ TTATCTGGAACATCTGTGGTATGG 3′	Tn*917* left, *ermB* intragenic primer
ltp-1	5′ AGAGAGATGTCACCGTCAAG 3′	Tn*917* left, outward-reading primer
ltp-2	5′ AATGTACAAAATAACAGCGAA 3′	Tn*917* left, outward-reading primer
rtp-1	5′ CTAAACACTTAAGAGAATTG 3′	Tn*917* right, outward-reading primer
rtp-2	5′ TAGGCCTTGAAACATTGGTT 3′	Tn*917* right, outward-reading primer
p1	5′ TGATTTCGTAGTCGCACCTCCG 3′	p*sagB*.KO.*erm* primer
p2-ascI	5′ GGCGCGCCCCCGCTTCATCTTGGCTGATTGAC 3′[a]	p*sagB*.KO.*erm* primer
Erm-PA	5′ GGCGCGCCCCGGGCCCAAAATTTGTTTGAT 3′[a]	p*sagB*.KO.*erm* primer
Erm-PB	5′ GGCCGGCCAGTCGGCAGCGACTCATAGAAT 3′[b]	p*sagB*.KO.*erm* primer
p3-ecoRI	5′ GGCCGGCCCACATTAGTAGGAAACAAGGAGTCG 3′[b]	p*sagB*.KO.*erm* primer
p4	5′ TAACTGGTTGCGTCGTTGG 3′	p*sagB*.KO.*erm* primer
SI *sagA* 1156	5′ ATTTGTATAAGGAGGTAAGC 3′	*S. iniae sagA* primer
SI *sagA* 1352	5′ AGTGAATTACTTTGGAGCTG 3′	*S. iniae sagA* primer
SK+	5′ GCTCTAGAACTAGTGG 3′	pVE6007Δ primer
T7	5′ TAATACGACTCACTATAGGG 3′	pVE6007Δ primer
sagA 1530	5′ ATGTTAAAATTTACTTC 3′	GAS *sagA* primer
sagA 1688	5′ TTTACCTGGCGTATAACTTC 3′	GAS *sagA* primer

[a] Underlining indicates *Asc*I site.
[b] Underlining indicates *Eco*RI site.

30 s, 45°C for 30 s, and 72° for 2 min; 30 cycles of 94°C for 30 s, 57°C for 30 s, and 72°C for 2 min; and 72°C for 7 min. Unique amplicons were gel purified with the QIAEX gel extraction kit (Qiagen) and sequenced by using the corresponding nested outward-reading primers, ltp-2 and rtp-2.

Southern localization of Tn*917*-junction fragments. Genomic DNA (~1 μg) was digested with *Hin*dIII, resolved by 0.6% Tris-borate-EDTA agarose gel electrophoresis, and transferred to a Nytran membrane. DNA probes, generated by PCR, were labeled by using the ECL direct nucleic acid labeling and detection system (Amersham Pharmacia Biotech, Quebec, Canada), and positive bands were visualized by chemiluminesence. SagA through SagHI probes were amplified from GAS NZ131 genomic DNA by using primers *sagA* 1530 and *sagA* 1688 (Table 2), as well as the *sagB*, *-C*, *-D*, *-E*, *-F*, *-G*, and *-HI* primer pairs described previously (38).

Targeted mutagenesis of *S. iniae sagB*. Targeted mutagenesis of *S. iniae sagB* was based on a recently described PCR ligation mutagenesis technique, which promotes insertion of heterologous DNA and deletion of target DNA (30). The chromosomal regions upstream (P12) and downstream (P34) of *S. iniae sagB* were amplified and ligated to the ERY resistance gene *ermB* (9) via *Asc*I and *Eco*RI restriction endonuclease sites, respectively, incorporated onto the 5′ ends of appropriate primers (Table 2). P12 (946 bp) was amplified by using a primer 630 bp upstream of *S. iniae sagA* (p1) and 65 bp downstream of *S. iniae sagB* (p2-ascI). Likewise, P34 (1,049 bp) was amplified by using a primer pair 23 bp upstream of the *S. iniae sagB* stop site (p3-ecoRI) and 807 bp downstream of the *S. iniae sagC* start codon (p4). The *ermB* product was amplified from the gene cassette (9) template and primers Erm-PA and Erm-PB (30), which have been described previously (Table 2). All three products were digested with *Asc*I and/or *Eco*RI and ligated. The 2,782-bp construct (P12::*erm*::P34) was amplified from the ligation mixture by using primers p1 and p4 and was cloned into the TA vector pCR2.1-TOPO. The insert was directionally cloned (*Xho*I/*Hin*dIII) into the temperature-sensitive shuttle vector pVE6007Δ, and the resultant plasmid, pSI*sagB*.KO.*erm*, was transformed into *S. iniae* 9117. CHL-resistant transformants were identified at the permissive temperature for plasmid replication (30°C). Single-crossover Campbell-type genomic insertions were selected by incubation at a nonpermissive temperature (37°C) while maintaining CHL selection. Selection was relaxed by serial passage at 30°C without antibiotics, and double-crossover events were identified by negative CHL selection (CHL-susceptible) in broth and the NH phenotype on SBA. Genomic DNA was examined for *ermB*, pVE6007Δ, and *sagB* by PCR and Southern hybridization. During mutant selection, it was apparent that SI *sagB*.KO.*erm* was sensitive to ERY selection. Sequencing of *ermB* from plasmid pSI*sagB*.KO.*erm* revealed a nucleotide deletion, downstream of the start site, which had created a premature TAA stop codon.

Complementation of SLS-negative GAS. By using primers SI *sagA* 1156 and SI *sagA* 1352, the entire *S. iniae sagA* locus, exclusive of the putative promoter, was amplified from *S. iniae* 9117 genomic DNA and TA-cloned into pCR2.1-TOPO. The insert was digested (*Eco*RV/*Bam*HI) and directionally cloned into the pDC123 shuttle vector, in the same orientation as the upstream *cat* promoter. The resultant construct, pSI*sagA*, was transformed into competent NZ131 *sagA*Δ*cat*. NZ131 *sagA*Δ*cat* is an NH, CHL resistant mutant of GAS strain NZ131 and harbors a precise, in-frame allelic replacement of the GAS *sagA* gene with the CHL acetyltransferase (*cat*) gene. This mutant was constructed by the same methodology described for mutagenesis of the *Streptococcus agalactiae* beta-hemolysin (43) with one exception: the temperature-sensitive targeting vector contained a GAS *sag* locus sequence where *sagA* was replaced by *cat* through in vivo PCR recombination. The nonpolarity of this mutant was confirmed by single-gene complementation to full wild-type SLS activity when GAS *sagA* was returned on a plasmid vector (V. Datta, R. G. Kansal, and V. Nizet, Abstr. 6th Ann. Streptococcal Genetics Conf. 2002, abstr. 132, p. 109, 2002).

Transformation of GAS strain NZ131 (wild type) and NZ131 *sagA*Δ*cat* with pDC123 alone provided appropriate experimental controls. Transformants were selected on SBA containing CHL (4 μg/ml), incubated both aerobically and anaerobically, and screened for a restored beta-hemolytic phenotype. Anaerobic incubation prevented alpha-hemolysis and potential misinterpretation of SLS-negative control strains. Plasmid DNA recovered from beta-hemolytic isolates was analyzed by PCR using primers SI *sagA* 1156 and SI *sagA* 1352.

Murine model of subcutaneous infection. The virulence of *S. iniae* strains was assessed by using a murine model of subcutaneous inoculation as previously described for GAS (4, 19). Mid-log-phase cultures were washed twice in phosphate-buffered saline (PBS), and 10^6 CFU was mixed with an equal volume of sterilized Cytodex beads (Sigma Chemical Co., St. Louis, Mo.) that were suspended in PBS to a concentration of 20 μg/ml. This mixture (200 μl) was injected into the right flanks of five to seven hairless, outbred female SKH1 mice (Charles River Laboratories, Wilmington, Mass.) aged 4 to 5 weeks, weighing 15 to 20 g. Mice were weighed prior to injection and every 24 h for 3 days. Blood was collected from a single mouse at 24 h and from the remaining mice at the end of each trial (72 h) by cardiac puncture and was mixed with citrate-buffered saline. Representative tissue samples at the injection site were removed from mice and homogenized in PBS. Viable counts were determined from both sample types. The experimental procedures performed on the mice were conducted according to the principles of the Animal Care Committee of Mount Sinai Hospital, Toronto, Ontario, Canada.

Phagocytosis assay. Resistance to phagocytosis in whole blood was examined by using a modified protocol of the Lancefield bactericidal assay for GAS (29). Mid-log-phase bacteria (10^8 CFU) were washed and serially diluted in PBS. Bacterial suspensions (100 μl) containing 10^2 to 10^4 CFU were added to 1 ml of fresh, heparinized human blood in sterile glass tubes and incubated on an orbital shaker for 1 h at 37°C. The survival index was calculated as the CFU recovered after 1 h of incubation divided by the initial inoculum added prior to incubation.

Hemolytic activity assay. The nature of *S. iniae* cytolysin activity was examined using a hemolysis assay based on the method previously described for SLS activity in GAS (4). Whole-cell and supernatant samples were collected from 1 ml of mid-log-phase cultures by centrifugation. Whole-cell fractions were washed three times and resuspended in 1 ml of PBS. A 1% sheep erythrocyte solution was prepared in PBS by using erythrocytes washed three times in the same buffer. Cell and supernatant samples (200 μl) were serially diluted across a 96-well round-bottom microtiter plate in THB, and 100 μl of sheep erythrocytes was added to each well. Plates were incubated for 1 h and centrifuged to pellet both erythrocytes and bacteria, and 100-μl aliquots of supernatant were transferred to a replica plate. The A_{450} was measured to determine the release of hemoglobin. Erythrocytes suspended in PBS plus 0.1% sodium dodecyl sulfate (complete lysis) or PBS alone (no lysis) were used as controls. Trypan blue (Sigma) at a final concentration of 13 μg/ml was used as an inhibitor of SLS activity.

Nucleotide sequence accession number. The nucleotide sequence data for the *S. iniae sag* gene cluster has been submitted to the DDBJ/EMBL/GenBank databases and was assigned accession number AF465842.

RESULTS

Cytolysin expression in *S. iniae*. Commensal and disease-associated strains were cultured on SBA under aerobic and anaerobic conditions. Regardless of oxygen tension, all 32 commensal strains exhibited pronounced zones of beta-hemolysis surrounding individual colonies. However, comparable zones of beta-hemolysis were observed with disease-associated strains (21) only when they were cultured anaerobically. Under aerobic conditions, disease-associated strains were largely alpha-hemolytic, with a weak zone of beta-hemolysis surrounding the colonies. Incubation beyond 24 h yielded a thin halo of beta-hemolysis between the colony and the zone of alpha-hemolysis, similar to the pattern originally described by Pier and Madin (42) (Fig. 1). Cytolytic activity, examined by using a hemolysis assay, was found to be associated with whole-cell preparations and could be inhibited by addition of the dye trypan blue (13 μg/ml), indicating SLS activity. Hemolytic activity was not observed in supernatants (data not shown).

Tn*917* mutagenesis and genomic sequence recovery. To identify the genomic region responsible for hemolysin expression in *S. iniae*, the single Tn*917* insertion sites in two NH mutants, SINH1 and SINH3, were mapped by Southern blot analysis. In SINH3, a 405-bp cloned *S. iniae* DNA fragment representing the transposon insertion site shared significant nucleotide similarity with the junction of the *sagG* and *sagH* genes from the SLS biosynthetic operon in GAS (Fig. 2). For SINH1, single-primer PCR analysis of flanking DNA revealed sequences with homology to the complete GAS *sagA* gene and part of the *sagB* gene, localizing the Tn*917* insertion to the region immediately downstream of the start codon of the homologue (Fig. 2).

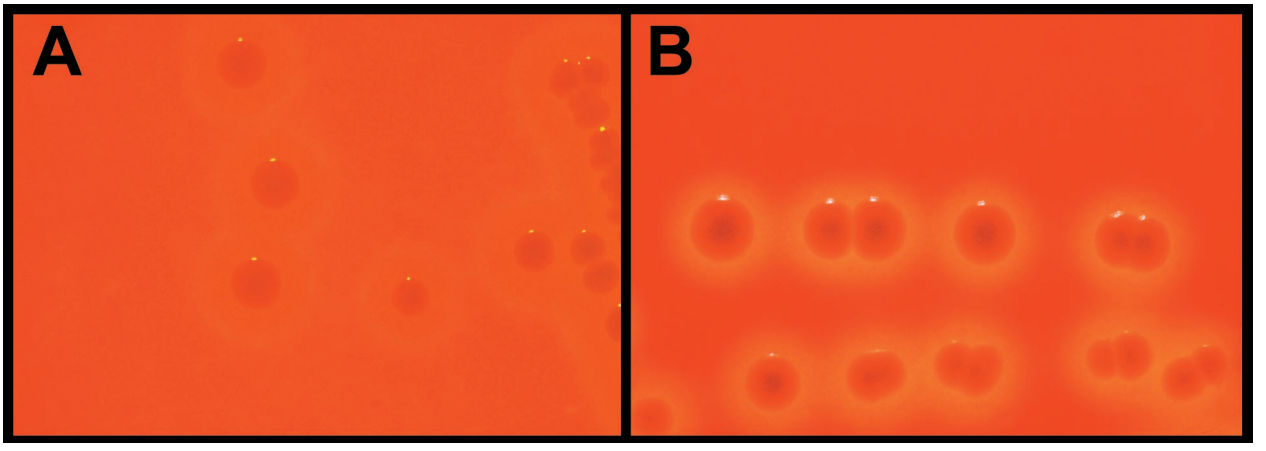

FIG. 1. Photograph depicting the hemolytic phenotypes exhibited by the disease-associated strain 9117 (A) and the commensal strain 9066 (B) of *S. iniae* cultured on SBA under aerobic conditions. Panel B is representative of the hemolysis exhibited by both disease-associated and commensal strains cultured anaerobically.

Characterization of the *sag*-like gene cluster in *S. iniae*. Southern hybridization with GAS-derived *sag* probes against *Hin*dIII-digested *S. iniae* genomic DNA indicated the presence of sequences in *S. iniae* homologous to each of the nine genes in the GAS *sag* operon. Additionally, the *S. iniae* genes appeared to be placed in the same genetic order as those in GAS (data not shown). The genomic DNA between the *S. iniae sagB* and *sagG* open reading frames (ORFs) (~4.5 kb) was amplified and sequenced through successive chromosomal walking steps. Sequence downstream of the *S. iniae sagG* ORF was obtained from a bacteriophage λ clone, generated in a concurrent study (C. Duncan, unpublished data) using the Lambda FIX II/*Xho*I Partial Fill-In Vector kit (Stratagene, La Jolla, Calif.), as identified by Southern hybridization with an *S. iniae sagG* probe. Oligonucleotide primers designed specifically for each of the nine *sag* ORFs of the disease-associated *S. iniae* strain 9117 yielded products of expected sizes from the representative commensal strain 9066. This finding indicated that conservation of the *sag*-like gene cluster in *S. iniae* was independent of the PFGE genetic profile associated with the capacity of the organism to produce invasive disease (48).

Sequence analysis of the *S. iniae sag*-like gene cluster. Table 3 lists the ORF sizes and homology with each of the corresponding GAS *sag* genes. The *S. iniae sagA* ORF encoded a predicted 54-amino-acid (aa) peptide exhibiting 73% sequence identity with SagA of GAS, which contains several features reminiscent of a bacteriocin prepropeptide (Fig. 3) (38). Conserved features of the two predicted SagA proteins include a putative leader peptide with a glycine-glycine cleavage site and a number of target residues (cysteine, serine, and glycine) in the proposed propeptide, which may serve as targets for posttranslational modification (Fig. 3).

The *S. iniae sagB* ORF encoded a predicted 316-aa product with 77% identity to SagB of GAS, and both of these products shared weak homology with the cytoplasmic modifying enzyme McbC of *E. coli* (20). McbC is involved in the posttranslational modification of McbA, to produce the mature bacteriocin microcin B17, and uses flavin mononucleotide (FMN) as a cofactor (36). A conserved domain in the SagB ORF of *S. iniae* (positions 125 to 298) was identified by using the conserved domain database (RPS-BLAST) in GenBank. By use of default parameters, the CDD search tool (GenBank) aligned 97% of this region to a group of nitroreductases (flavoproteins) that bind FMN noncovalently (Fig. 4). The NADH oxidase (NO) of *Thermus thermophilus* and the nitroreductase (NR) of *Enterobacter cloacae* align most closely with *S. iniae* SagB (7, 40).

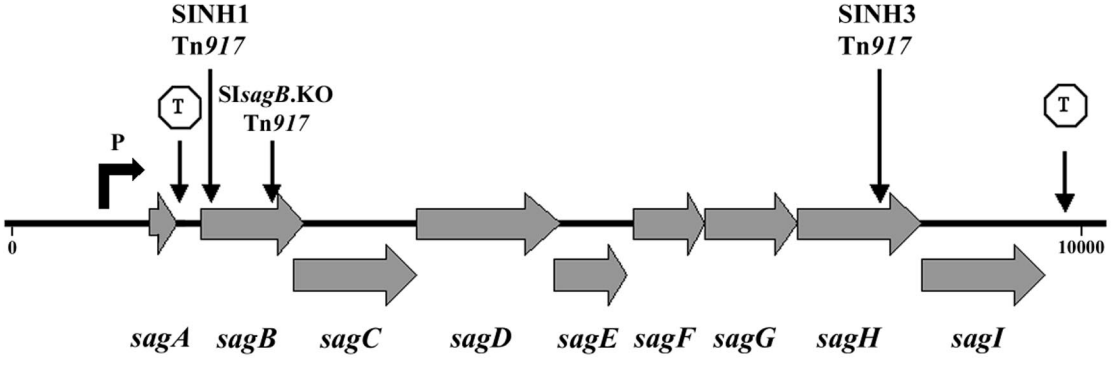

FIG. 2. Map of *S. iniae* SLS-associated gene cluster. Tn*917* insertion points of characterized mutants (SINHI, SINH3, and SI *sagB*.KO.Tn*917*), and the putative promoter (P) and rho-independent terminator (T) regions, are indicated.

TABLE 3. Predicted Sag proteins in *S. iniae*

Gene	Protein length (aa)	% Identity (% similarity) to GAS Sag products
sagA	54	73 (80)
sagB	316	77 (85)
sagC	354	78 (87)
sagD	453	82 (87)
sagE	220	60 (75)
sagF	229	52 (70)
sagG	307	75 (84)
sagH	375	81 (89)
sagI	372	74 (84)

Several residues, Ser^{46}, Pro^{156}, Leu^{158}, and Gly^{159} of *T. thermophilus*, are directly associated with FMN binding (24) and, along with neighboring residues, are relatively conserved in this family of flavoproteins (47). These putative FMN-binding regions are also relatively conserved in the *S. iniae* and GAS SagB proteins and *E. coli* McbC, specifically Ser^{46} and Gly^{159} residues (Fig. 4).

The *sagC*, *sagD*, *sagE*, and *sagF* ORFs of *S. iniae* encoded predicted products with significant amino acid identity to corresponding *sag* products of GAS yet shared no homology with other proteins in the GenBank database. As reported for GAS, the SagG, SagH, and SagI predicted proteins of *S. iniae* exhibited homology to the components of a family of ATP-binding cassette (ABC)-type transport systems. These products showed the greatest homology (47, 22, and 23% amino acid identity, respectively) to the ABC transport system expressed by *Clostridium acetobutylicum* (39). By use of the CDD search tool (RPS-BLAST) in GenBank, 58% (positions 30 to 210) of the predicted SagG-like protein structure was found to be completely conserved with the ATPase component of the ABC transporter protein family mentioned above. Inverted-repeat stem sequences consistent with rho-independent terminators were found between the *sagA and sagB* ORFs and immediately downstream of the *sagI* ORF of *S. iniae* (Fig. 2), similar to those reported for GAS (38).

Targeted mutagenesis of the *S. iniae sagB* locus. Each of the nine *sag* operon genes appears to be required for SLS expression in GAS (38). We chose targeted mutagenesis of *S. iniae sagB* to confirm the role of the *S. iniae sag* locus in SLS expression and to accurately assess the role of SLS in *S. iniae* virulence. A plasmid was constructed for deletion of *S. iniae sagB* and insertion of *ermB*, by double-crossover recombination, using the temperature-sensitive vector pVE6007Δ. The plasmid, pSI*sagB*.KO.*erm*, was transformed into *S. iniae* 9117, and cultures were monitored for evidence of plasmid integration (i.e., isolates growing on CHL at the nonpermissive temperature for pVE6007Δ). Single-crossover events were identified by PCR using *ermB* and pVE6007Δ primers (SK+ and T7). Insertional mutants were continually subcultured at permissive temperatures to enable pVE6007Δ excision from the chromosome during homologous recombination. Following ~6 subcultures, a CHL-sensitive, NH isolate was recovered. PCR indicated that the mutant, SI *sagB*.KO.*erm*, had retained the *ermB* gene but had lost the pVE6007Δ vector backbone. The *ermB* probe hybridized with the expected 6.0-kb region in both single- and double-crossover mutants (Fig. 5A). Conversely, pVE6007Δ hybridized with the expected 6.0-kb region in the single-crossover mutant only, indicating pVE6007Δ excision from SI *sagB*.KO.*erm*. Moreover, only the single-crossover mutant hybridized with a probe generated from *S. iniae sagB* (Fig. 5C). Collectively, these results indicated that the loss of the hemolytic phenotype in SI *sagB*.KO.*erm* could be attributed to the replacement of *S. iniae sagB* by *ermB*.

Restoration of hemolysis in SLS-negative GAS by use of the *S. iniae sagA* locus. To determine whether the *S. iniae sagA* gene encodes a functional homologue of the putative GAS SLS precursor, the NH GAS allelic replacement mutant, NZ131 *sagA*Δ*cat*, was transformed with *S. iniae sagA* (pSI*sagA*). Transformants exhibited a restored beta-hemolytic phenotype whether grown aerobically or anaerobically (Fig. 6), while the mutant strain transformed with the vector alone remained NH. The extent of beta-hemolysis exhibited by the complemented mutant NZ131 *sagA*Δ*cat*(pSI*sagA*) was comparable to that observed for the wild-type GAS strain, NZ131, transformed with the vector alone. Thus, the *sagA* gene of *S. iniae* was sufficient to restore the SLS phenotype in a *sagA* mutant of GAS.

Virulence of SI *sagB*.KO.*erm* in a murine model. Mice infected with 10^6 CFU of SI *sagB*.KO.*erm* showed signs of lethargy and wasting similar to those of mice infected with the wild type at 24 h postinoculation. Similarly, a median weight loss of 4.3 g (range, 2.0 to 6.5 g), comparable to that of mice infected with the wild type (5.0 g; range, 2.0 to 5.5 g), was noted (Fig. 7).

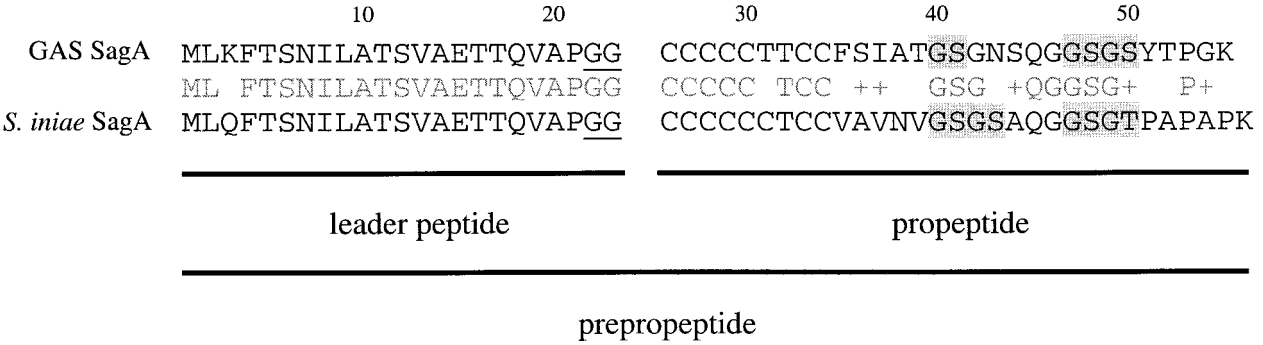

FIG. 3. Amino acid sequence similarity between SagA proteins of *S. iniae* and GAS. Putative Gly-Gly cleavage sites are underlined, and residues thought to undergo posttranslational modification are shaded.

		*		*
S. iniae SagB	170	LRN**CASG**GGLYPI	277	AYGSV**DIGGY**SKEY
S. pyogenes SagB	170	LRN**CASG**GGLYPI	277	TYGSI**DIGGY**NKEY
E. cloacae NR	40	LQY**SPSS**TNSQPW	151	GLDAV**PIEGF**DAAI
T. thermophilus NO	34	ALR**APSA**WNLQUW	157	GLGSV**PMLGF**DPER
E. coli McbC	117	RRP**YPSG**GALYPI	229	GLKNR**VWAGY**TDSY
S. epidermidis EpiD	31	ILF**SPSS**KNFINT		

FIG. 4. Amino acid alignment of putative FMN-binding regions of bacterial flavoproteins and SagB. Sequences are derived from the NR of *E. cloacae*, NO of *T. thermophilus*, and bacteriocin-processing enzymes McbC and EpiD from *E. coli* and *S. epidermidis*, respectively. Asterisks indicate conserved residues. Residues directly bound to FMN in *T. thermophilus* NO are underlined. Boldfaced residues represent putative FMN-binding regions.

Mice infected with SI *sagB*.KO.*erm* (10^6 CFU) maintained significant bacteremia over the 72-h trial. One mouse, euthanatized at 24 h postinoculation, harbored 10^5 CFU/ml in the blood, and 10^4 to 10^5 CFU/ml was recovered from the blood of the remaining six mice at 72 h. Similar levels of bacteria were recovered from mice infected with the wild-type strain 9117. SI *sagB*.KO.*erm* was capable of causing bacteremia (10^5 CFU/ml) from an inoculum as low as 10^2 CFU, as previously reported for strain 9117 (19). Bacteria isolated from the blood of SI *sagB*.KO.*erm*-infected mice remained NH under anaerobic culture conditions, confirming the integrity of the mutant phenotype.

Although the commensal strain 9066 does not induce invasive disease in mice, even at an inoculum as high as 10^8 CFU (19), it does give rise to a localized necrotic lesion at the site of inoculation, as does the disease-associated strain 9117. However, with the latter, mortality due to bacteremia occurs rapidly and progression of the necrotic lesion cannot be monitored. In order to examine the role of SLS in necrotic-lesion formation, we used the NH commensal mutant SI *sagB*.KO.Tn*917*, which contains a Tn*917* insertion within the *sagB* ORF, in the murine model. Mice were inoculated either with 10^8 CFU of SI *sagB*.KO.Tn*917* or with one of the wild-type strains 9174 and 9066. Strain 9174 caused necrotic lesions in 60% (3 of 5) of mice, compared to 100% (5 of 5) necrotic-lesion formation in 9066-infected mice. In contrast, SI *sagB*.KO.Tn*917* did not cause necrotic lesions in mice ($n = 5$). Mice inoculated with 9066, 9174, or SI *sagB*.KO.Tn*917* all experienced weight gains, with medians of 1.0 g (range, 0.0 to 2.5 g), 1.25 g (range, 1.0 to 3.0 g) and 0.25 g (range, 0.0 to 1.0 g), respectively, as did those inoculated with Cytodex and no bacteria (1.0 g; range, 0.0 to 2.5 g) ($P = 0.95$ by the Wilcoxon signed-rank test). None of these mice developed bacteremia. Culture of the inoculation site from SI *sagB*.KO.Tn*917*-inoculated mice yielded NH colonies on SBA with or without ERY, confirming the stability of the mutant in vivo.

Effect of SLS expression on *S. iniae* resistance to phagocytosis. Disease-associated strains of *S. iniae* have been found to be highly resistant to killing by human blood, in contrast to the marked susceptibility of commensal isolates (19). Following exposure of the NH mutant SI *sagB*.KO.*erm* to whole human blood, the number of viable CFU recovered (percent survival) was comparable to that for the wild-type disease-associated strain 9117. As shown in Fig. 8, 75% of the SI *sagB*.KO.*erm* inoculum was recovered from blood, in comparison to 79% recovery of 9117. In contrast, the commensal isolate 9066 was completely susceptible to whole-blood killing, as previously described (19).

DISCUSSION

Disease-associated strains of *S. iniae*, represented by a unique genetic profile, cause soft-tissue infection in humans and are able to sustain invasive disease in a murine model of soft-tissue infection (19). However, the precise bacterial factors contributing to disease have not been elucidated. We hypothesized that the *S. iniae* cytolysin, responsible for its hemolytic phenotype, may represent one such virulence determinant. Insertional mutagenesis of a disease-associated strain of *S. iniae* and subsequent sequencing steps led to the discovery

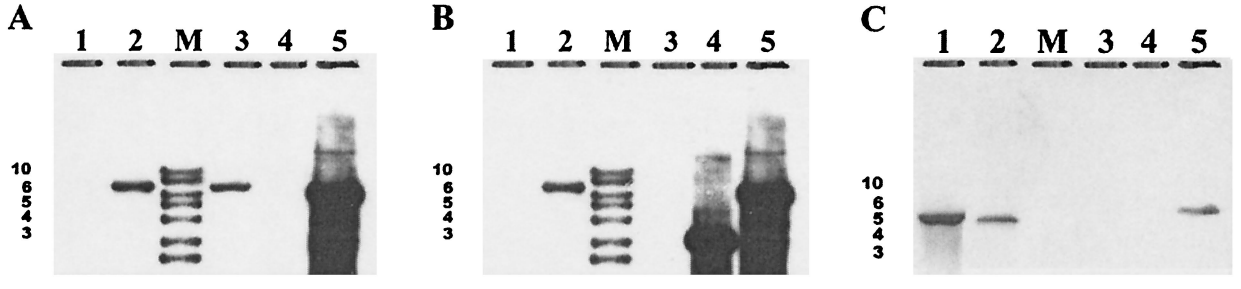

FIG. 5. Southern blot analysis of pSI*sagB*.KO.*erm* recombination into the *S. iniae* 9117 genome. Each lane represents *Hin*dIII-digested genomic or plasmid DNA. Lanes: 1, wild type; 2, single-crossover mutant; M, marker; 3, double-crossover mutant; 4, pVE6007Δ (control); 5, pSI*sagB*.KO.*erm* (control). Probes were *ermB* (A), pVE6007Δ (B), and *sagB* from *S. iniae* (C). Molecular sizes (in kilobases) are indicated to the left of each image.

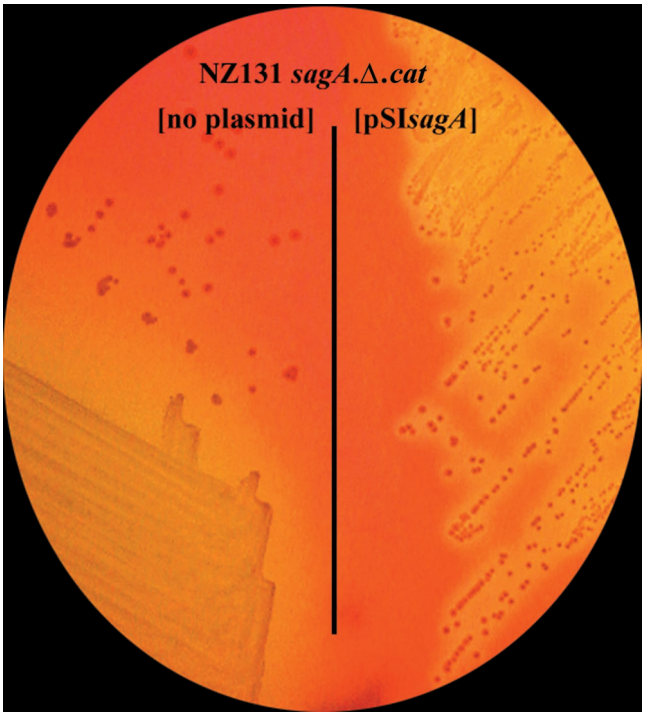

FIG. 6. Photograph illustrating restoration of the SLS phenotype in the NH GAS mutant NZ131 *sagA*Δ*cat* (left) following complementation with pSI*sagA*, harboring the *sagA* ORF from the disease-associated *S. iniae* strain 9117 (right). Cultures were incubated anaerobically at 37°C.

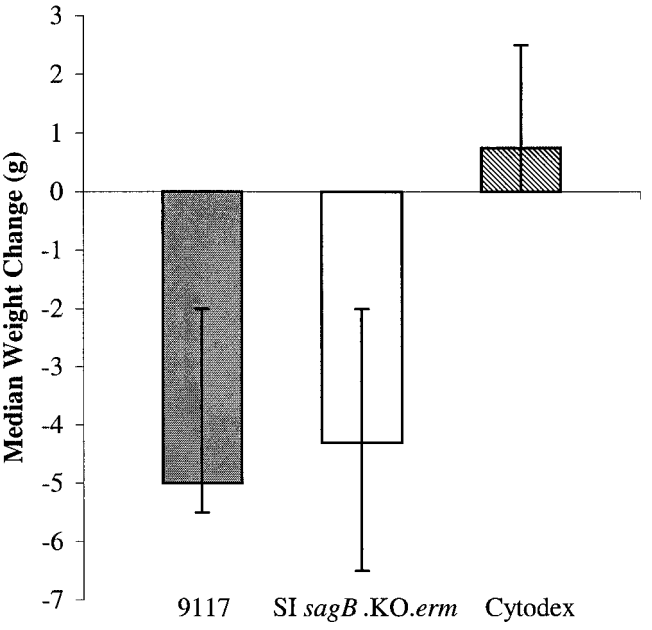

FIG. 7. Weight change observed in hairless female mice 72 h after subcutaneous inoculation with strains of *S. iniae*. Bars represent median weight gains ± ranges. Mice infected with the disease-associated *S. iniae* strain 9117 (shaded bar) or the *sagB* mutant (open bar) experienced significant weight loss, in contrast to a weight gain observed for mice inoculated with sterile Cytodex and no bacteria (striped bar) (0.75 g; range, 0.0 to 2.5 g) ($P < 0.005$ by the Wilcoxon signed-rank test).

that *S. iniae* cytolytic activity is encoded by a gene cluster that shares significant genetic similarities with the 9-gene GAS *sag* operon for SLS biosynthesis (38). The first gene of this operon, *sagA*, encodes a putative bacteriocin-like prepropeptide with sequence similarity to the microcin B17 precursor (McbA) from *E. coli*. Immunological studies have recently provided convincing evidence that *sagA* is the structural gene encoding SLS. Antibodies raised against a synthetic peptide of SagA effectively abolished the cytolytic activity of SLS (10). The remaining gene products of the operon are contiguously aligned (*sagB to sagI*) and are considered important for the processing and transport of SagA. In addition, while the GAS *sag* operon is both necessary and sufficient for SLS production, there is evidence that *sagA* may also possess a regulatory function affecting the expression of SLS and other GAS virulence factors through a complex mechanism (6, 32, 34).

The discovery of an SLS homologue in *S. iniae* adds to a small list of streptococcal pathogens harboring a version of this potent exotoxin. Human large-colony, beta-hemolytic group C and group G streptococci, belonging to *Streptococcus equisimilis* subsp. *dysgalactiae*, were recently shown to possess *sag*-like genetic loci for SLS biosynthesis (25). *Streptococcus equi*, the cause of strangles in horses, produces a beta-hemolysin with SLS-like characteristics (15). SLS is distinct from the other GAS hemolysin, SLO, a cholesterol-dependent, oxygen-labile cytolysin encoded by a single gene (21, 27), and the beta-hemolysin/cytolysin of GBS, encoded by the *cylE* gene (43, 45).

Comparative analysis between the GAS and *S. iniae sag* clusters revealed significant amino acid similarity and an identical gene arrangement. Additional features shared with GAS were a putative promoter region upstream of the *sagA* ORF, ribosomal binding sites and translational stop codons for each gene, and two noncoding regions that harbor putative rho-independent terminators, located between the *sagA* and *sagB*

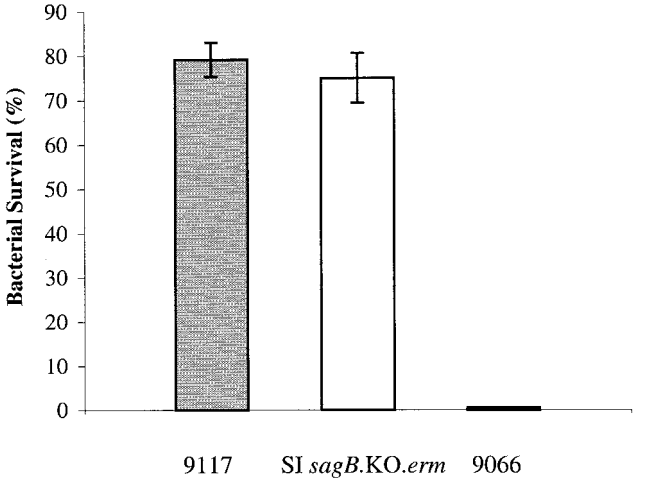

FIG. 8. Resistance to phagocytosis of the disease-associated *S. iniae* strain 9117 (shaded bar), the *sagB* mutant (open bar), and the commensal strain 9066 (solid bar) in whole blood. Each bar represents the percentage of viable organisms relative to the initial inoculum (100%) remaining after 1.0 h of rotation in fresh human blood. Results are means ± standard deviations.

ORFs and downstream of the *sagI* ORF (38). Residues that are considered important for SagA maturation in GAS are conserved in *S. iniae*. The Gly-Gly sequence is thought to precede a cleavage site that would remove the putative leader sequence and yield a product equivalent to the predicted size of SLS in GAS (38). The propeptide sequence of *S. iniae* also contains a high number of residues (8 cysteines, 3 serines, and 5 glycines) that are considered precursors for posttranslational modification in GAS SagA (38). Complementation and trypan blue inhibition studies demonstrated the functional relatedness of the *sagA* gene products. When the *sagA* locus of *S. iniae* was cloned and transformed into a *sagA* allelic replacement mutant of GAS, cytolytic activity was restored. Therefore, these findings demonstrate that, in addition to conserved amino acid sequence, the biological activities of the SagA peptides are similar and that the additional proteins required for processing and/or transport of SLS do not discriminate between these two SagA peptides.

The SagB product of *S. iniae* contains a protein domain conserved among a group of bacterial flavoproteins, most notably the NR of *E. cloacae* and the NO of *T. thermophilus* (7, 40). Furthermore, the FMN-binding regions of *T. thermophilus* NO (24) are potentially conserved in other flavoproteins (47) as well as SagB. The amino acid sequences of the SagB products also share weak homology with McbC of *E. coli* (20). In conjunction with McbB and McbD, McbC forms the microcin B17 synthetase that directs the chemical modification of McbA prepropeptide amino acids (31). Interestingly, preliminary studies have suggested that McbC is a flavoprotein in that recombinant protein is associated with stoichiometric quantities of FMN (36). The bacteriocin epidermin, produced by *Staphylococcus epidermidis*, also requires the enzymatic action of a flavoprotein, EpiD, for posttranslational modification (28). In addition, at least one of the conserved FMN-binding motifs mentioned above is present in both McbC and EpiD. These observations, in combination with the predicted cytoplasmic localization of SagB (38), support the hypothesis that these conserved regions in SagB are involved in FMN binding and that SagB contributes to the chemical modification of SagA. Liu et al. reported elimination of SLS activity in a transposon Tn*916* mutant of GAS deficient in riboflavin biosynthesis (34). Considering that FMN is a direct product of riboflavin metabolism, a requirement for FMN would provide the link between SLS activity and riboflavin biosynthesis.

Although the *S. iniae* cytolysin confers a beta-hemolytic phenotype on SBA, the hemolytic profile of disease-associated strains is less profound than that of commensal strains when cultures are grown aerobically. In vitro growth exhibits weak beta-hemolysis encircling a zone of alpha-hemolysis and can easily be confused with the alpha-hemolysis of viridans streptococcal species. Yet the extent of cytolysis is equivalent when disease-associated and commensal strains are cultured anaerobically. The nucleotide sequence of *sagA*, including the promoter region and >600 bp upstream of the *sagA* ORF, is identical in disease-associated and commensal isolates (data not shown). Following complementation of an NH strain of GAS with the *S. iniae sagA* gene from a disease-associated strain, a beta-hemolytic phenotype resulted, regardless of oxygen tension. These findings suggest that a regulatory mechanism, rather than structural differences in SagA, affects the oxygen-dependent expression of SLS in disease-associated strains. In GAS, the CovR-CovS two-component regulatory system and the negative regulators Nra and RofA negatively influence *sagA* transcription (2, 14, 37), and *rofA* is also affected by oxygen conditions (16, 17). A small number of strains expressing hemolytic phenotypes opposite to those described for their genotypes (disease associated versus commensal) have been identified. These include two commensal strains and the ATCC type strain 29178, expressing the alpha/beta-hemolytic phenotype, as well as two constitutively beta-hemolytic disease-associated strains, all grown under aerobic and anaerobic conditions (data not shown). Although the selective advantage that this oxygen-dependent SLS phenotype confers on *S. iniae* is not immediately apparent, these observations lend further support to the hypothesis that SLS expression is under some degree of regulation.

By use of a murine model of subcutaneous infection, SLS activity in GAS has been linked to tissue necrosis (4). Recent work showed that targeted mutagenesis of each of the *sag* genes generated an NH mutant, while mutagenesis immediately downstream of the operon did not abolish hemolysis, demonstrating a direct link between the hemolytic phenotype and the defined *sag* locus (38). When a GAS *sagA* allelic replacement mutant (NZ131 *sagA*Δ*cat*) was examined in a murine model of subcutaneous infection, a complete attenuation of necrotic-lesion formation, similar to that in previous studies (4), was observed (unpublished data), emphasizing the importance of *sagA* expression in GAS virulence. By using a disease-associated strain of *S. iniae*, a *sagB* insertion-deletion mutant was generated to examine the role of SLS in the virulence of this pathogen. Previous work with *S. iniae* demonstrated that disease-associated strains, in stark contrast to commensal isolates, established bacteremic infection in the murine model following subcutaneous inoculation and were highly resistant to phagocytic killing in whole human blood (19). Interestingly, the SLS-deficient SI *sagB*.KO.*erm* mutant was also able to cause invasive disease in this model, even at low inocula, with no evident signs of attenuated virulence in comparison to that with the wild type. Furthermore, this mutant remained resistant to whole-blood killing in vitro. From these studies, it is apparent that the contribution of *S. iniae* SLS to bacteremia and resistance to phagocytosis is negligible. It was previously reported that disease-associated and commensal strains of *S. iniae* can elicit localized necrosis in the murine model, similar to that elicited by GAS, if a higher inoculum of 10^8 CFU is used (19). However, mice infected with disease-associated strains at this dose are at risk of terminal disease, likely due to the invasiveness of these strains. Thus, we examined necrotic-lesion formation caused by a commensal isolate and its SLS-deficient counterpart. In contrast to the commensal wild-type isolate, which caused necrotic lesions in 60% of animals, the SLS-deficient mutant, SI *sagB*.KO.Tn*917*, did not cause localized cell damage in mice. These results suggest that SLS of *S. iniae* contributes to tissue damage but not to bacteremia.

In summary, we have identified an SLS-associated gene cluster within the chromosome of *S. iniae* with strong homology to that of GAS and demonstrated the requirement for SLS in causing tissue damage in a mammalian model. While SLS does seem to contribute to virulence by promoting local tissue ne-

crosis, it does not play a critical role in the establishment of bacteremia in mice. However, *S. iniae* infection in fish is characterized by meningoencephalitis, and SLS may be required for brain endothelial-cell injury. Future studies will test this hypothesis in a fish infection model of meningoencephalitis.

ACKNOWLEDGMENT

This work was supported by a grant from the Canadian Bacterial Diseases Network.

REFERENCES

1. **Altschul, S. F., W. Gish, W. Miller, E. W. Myers, and D. J. Lipman.** 1990. Basic local alignment search tool. J. Mol. Biol. **215:**403–410.
2. **Beckert, S., B. Kreikemeyer, and A. Podbielski.** 2001. Group A streptococcal *rofA* gene is involved in the control of several virulence genes and eukaryotic cell attachment and internalization. Infect. Immun. **69:**534–537.
3. **Berry, A. M., J. Yother, D. E. Briles, D. Hansman, and J. C. Paton.** 1989. Reduced virulence of a defined pneumolysin-negative mutant of *Streptococcus pneumoniae*. Infect. Immun. **57:**2037–2042.
4. **Betschel, S. D., S. M. Borgia, N. L. Barg, D. E. Low, and J. C. S. de Azavedo.** 1998. Reduced virulence of group A streptococcal Tn*916* mutants that do not produce streptolysin S. Infect. Immun. **66:**1671–1679.
5. **Birnboim, H. C., and J. Doly.** 1979. A rapid alkaline extraction procedure for screening recombinant plasmid DNA. Nucleic Acids Res. **7:**1513–1523.
6. **Biswas, I., P. Germon, K. McDade, and J. R. Scott.** 2001. Generation and surface localization of intact M protein in *Streptococcus pyogenes* are dependent on *sagA*. Infect. Immun. **69:**7029–7038.
7. **Bryant, C., L. Hubbard, and W. D. McElroy.** 1991. Cloning, nucleotide sequence, and expression of the nitroreductase gene from *Enterobacter cloacae*. J. Biol. Chem. **266:**4126–4130.
8. **Chaffin, D. O., and C. E. Rubens.** 1998. Blue/white screening of recombinant plasmids in Gram-positive bacteria by interruption of alkaline phosphatase gene (*phoZ*) expression. Gene **219:**91–99.
9. **Claverys, J. P., A. Dintilhac, E. V. Pestova, B. Martin, and D. A. Morrison.** 1995. Construction and evaluation of new drug-resistance cassettes for gene disruption mutagenesis in *Streptococcus pneumoniae*, using an ami test platform. Gene **164:**123–128.
10. **Dale, J. B., E. Y. Chiang, D. L. Hasty, and H. S. Courtney.** 2002. Antibodies against a synthetic peptide of SagA neutralize the cytolytic activity of streptolysin S from group A streptococci. Infect. Immun. **70:**2166–2170.
11. **Dower, W. J., J. F. Miller, and C. W. Ragsdale.** 1988. High efficiency transformation of *Escherichia coli* by high voltage electroporation. Nucleic Acids Res. **16:**6127–6145.
12. **Eldar, A., Y. Bejerano, and H. Bercovier.** 1994. *Streptococcus shiloi* and *Streptococcus difficile*: two new streptococcal species causing a meningoencephalitis in fish. Curr. Microbiol. **28:**139–143.
13. **Eldar, A., P. F. Frelier, L. Assenta, P. W. Varner, S. Lawhon, and H. Bercovier.** 1995. *Streptococcus shiloi*, the name for an agent causing septicemic infection in fish, is a junior synonym of *Streptococcus iniae*. Int. J. Syst. Bacteriol. **45:**840–842.
14. **Federle, M. J., K. S. McIver, and J. R. Scott.** 1999. A response regulator that represses transcription of several virulence operons in the group A streptococcus. J. Bacteriol. **181:**3649–3657.
15. **Flanagan, J., N. Collin, J. Timoney, T. Mitchell, J. A. Mumford, and N. Chanter.** 1998. Characterization of the haemolytic activity of *Streptococcus equi*. Microb. Pathog. **24:**211–221.
16. **Fogg, G. C., and M. G. Caparon.** 1997. Constitutive expression of fibronectin binding in *Streptococcus pyogenes* as a result of anaerobic activation of *rofA*. J. Bacteriol. **179:**6172–6180.
17. **Fogg, G. C., C. M. Gibson, and M. G. Caparon.** 1994. The identification of *rofA*, a positive-acting regulatory component of *prtF* expression: use of an m gamma delta-based shuttle mutagenesis strategy in *Streptococcus pyogenes*. Mol. Microbiol. **11:**671–684.
18. **Framson, P., A. Nittayajarn, J. Merry, P. Youngman, and C. E. Rubens.** 1997. New genetic techniques for group B streptococci: high-efficiency transformation, maintenance of temperature-sensitive pWV01 plasmids, and mutagenesis with Tn*917*. Appl. Environ. Microbiol. **63:**3539–3547.
19. **Fuller, J. D., D. J. Bast, V. Nizet, D. E. Low, and J. C. S. de Azavedo.** 2001. *Streptococcus iniae* virulence is associated with a distinct genetic profile. Infect. Immun. **69:**1994–2000.
20. **Genilloud, O., F. Moreno, and R. Kolter.** 1989. DNA sequence, products, and transcriptional pattern of the genes involved in production of the DNA replication inhibitor microcin B17. J. Bacteriol. **171:**1126–1135.
21. **Ginsberg, I.** 1970. Streptolysin S, p. 99–171. *In* T. C. Montie, S. Kadis, and S. J. Ajl (ed.), Microbial toxins, vol. 3. Bacterial protein toxins. Academic Press, New York, N.Y.
22. **Grant, S. G., J. Jessee, F. R. Bloom, and D. Hanahan.** 1990. Differential plasmid rescue from transgenic mouse DNAs into *Escherichia coli* methylation-restriction mutants. Proc. Natl. Acad. Sci. USA **87:**4645–4649.
23. **Gutierrez, J. A., P. J. Crowley, D. P. Brown, J. D. Hillman, P. Youngman, and A. S. Bleiweis.** 1996. Insertional mutagenesis and recovery of interrupted genes of *Streptococcus mutans* by using transposon Tn*917*: preliminary characterization of mutants displaying acid sensitivity and nutritional requirements. J. Bacteriol. **178:**4166–4175.
24. **Hecht, H. J., H. Erdmann, H. J. Park, M. Sprinzl, and R. D. Schmid.** 1995. Crystal structure of NADH oxidase from *Thermus thermophilus*. Nat. Struct. Biol. **2:**1109–1114.
25. **Humar, D., V. Datta, D. J. Bast, B. Beall, J. C. S. De Azavedo, and V. Nizet.** 2002. Streptolysin S and necrotising infections produced by group G streptococcus. Lancet **359:**124–129.
26. **Karlyshev, A. V., M. J. Pallen, and B. W. Wren.** 2000. Single-primer PCR procedure for rapid identification of transposon insertion sites. BioTechniques **28:**1078, 1080, 1082.
27. **Kehoe, M., and K. N. Timmis.** 1984. Cloning and expression in *Escherichia coli* of the streptolysin O determinant from *Streptococcus pyogenes*: characterization of the cloned streptolysin O determinant and demonstration of the absence of substantial homology with determinants of other thiol-activated toxins. Infect. Immun. **43:**804–810.
28. **Kupke, T., M. Uebele, D. Schmid, G. Jung, M. Blaesse, and S. Steinbacher.** 2000. Molecular characterization of lantibiotic-synthesizing enzyme EpiD reveals a function for bacterial Dfp proteins in coenzyme A biosynthesis. J. Biol. Chem. **275:**31838–31846.
29. **Lancefield, R. C.** 1962. Current knowledge of the type-specific M antigens of group A streptococci. J. Immunol. **89:**307–313.
30. **Lau, P. C., C. K. Sung, J. H. Lee, D. A. Morrison, and D. G. Cvitkovitch.** 2002. PCR ligation mutagenesis in transformable streptococci: application and efficiency. J. Microbiol. Methods **49:**193–205.
31. **Li, Y. M., J. C. Milne, L. L. Madison, R. Kolter, and C. T. Walsh.** 1996. From peptide precursors to oxazole and thiazole-containing peptide antibiotics: microcin B17 synthase. Science **274:**1188–1193.
32. **Li, Z., D. D. Sledjeski, B. Kreikemeyer, A. Podbielski, and M. D. Boyle.** 1999. Identification of *pel*, a *Streptococcus pyogenes* locus that affects both surface and secreted proteins. J. Bacteriol. **181:**6019–6027.
33. **Limbago, B., V. Penumalli, B. Weinrick, and J. R. Scott.** 2000. Role of streptolysin O in a mouse model of invasive group A streptococcal disease. Infect. Immun. **68:**6384–6390.
34. **Liu, S., S. Sela, G. Cohen, J. Jadoun, A. Cheung, and I. Ofek.** 1997. Insertional inactivation of streptolysin S expression is associated with altered riboflavin metabolism in *Streptococcus pyogenes*. Microb. Pathog. **22:**227–234.
35. **Maguin, E., P. Duwat, T. Hege, D. Ehrlich, and A. Gruss.** 1992. New thermosensitive plasmid for gram-positive bacteria. J. Bacteriol. **174:**5633–5638.
36. **Milne, J. C., R. S. Roy, A. C. Eliot, N. L. Kelleher, A. Wokhlu, B. Nickels, and C. T. Walsh.** 1999. Cofactor requirements and reconstitution of microcin B17 synthetase: a multienzyme complex that catalyzes the formation of oxazoles and thiazoles in the antibiotic microcin B17. Biochemistry **38:**4768–4781.
37. **Molinari, G., M. Rohde, S. R. Talay, G. S. Chhatwal, S. Beckert, and A. Podbielski.** 2001. The role played by the group A streptococcal negative regulator Nra on bacterial interactions with epithelial cells. Mol. Microbiol. **40:**99–114.
38. **Nizet, V., B. Beall, D. J. Bast, V. Datta, L. Kilburn, D. E. Low, and J. C. S. de Azavedo.** 2000. Genetic locus for streptolysin S production by group A streptococcus. Infect. Immun. **68:**4245–4254.
39. **Nolling, J., G. Breton, M. V. Omelchenko, K. S. Makarova, Q. Zeng, R. Gibson, H. M. Lee, J. Dubois, D. Qiu, J. Hitti, Y. I. Wolf, R. L. Tatusov, F. Sabathe, L. Doucette-Stamm, P. Soucaille, M. J. Daly, G. N. Bennett, E. V. Koonin, and D. R. Smith.** 2001. Genome sequence and comparative analysis of the solvent-producing bacterium *Clostridium acetobutylicum*. J. Bacteriol. **183:**4823–4838.
40. **Park, H. J., R. Kreutzer, C. O. Reiser, and M. Sprinzl.** 1993. Molecular cloning and nucleotide sequence of the gene encoding a H_2O_2-forming NADH oxidase from the extreme thermophilic *Thermus thermophilus* HB8 and its expression in *Escherichia coli*. Eur. J. Biochem. **211:**909.
41. **Perera, R. P., S. K. Johnson, M. D. Collins, and D. H. Lewis.** 1994. *Streptococcus iniae* associated with mortality of *Tilapia nilotica* × *T. aurea* hybrids. J. Aquat. Anim. Health **6:**335–340.
42. **Pier, G. B., and S. H. Madin.** 1976. *Streptococcus iniae* sp. nov., a beta-hemolytic streptococcus isolated from an Amazon freshwater dolphin, *Inia geoffrensis*. Int. J. Syst. Bacteriol. **26:**545–553.
43. **Pritzlaff, C. A., J. C. Chang, S. P. Kuo, G. S. Tamura, C. E. Rubens, and V. Nizet.** 2001. Genetic basis for the beta-haemolytic/cytolytic activity of group B Streptococcus. Mol. Microbiol. **39:**236–247.
44. **Simon, D., and J. J. Ferretti.** 1991. Electrotransformation of *Streptococcus pyogenes* with plasmid and linear DNA. FEMS Microbiol. Lett. **66:**219–224.
45. **Spellerberg, B., B. Pohl, G. Haase, S. Martin, J. Weber-Heynemann, and R. Lutticken.** 1999. Identification of genetic determinants for the hemolytic activity of *Streptococcus agalactiae* by ISS1 transposition. J. Bacteriol. **181:**3212–3219.
46. **Vriesema, A. J. M., S. A. J. Zaat, and J. Dankert.** 1996. A simple procedure

for isolation of cloning vectors and endogenous plasmids from viridans group streptococci and *Staphylococcus aureus*. Appl. Environ. Microbiol. **62:**3527–3529.

47. **Watanabe, M., T. Nishino, K. Takio, T. Sofuni, and T. Nohmi.** 1998. Purification and characterization of wild-type and mutant "classical" nitroreductases of *Salmonella typhimurium*. L33R mutation greatly diminishes binding of FMN to the nitroreductase of *S. typhimurium*. J. Biol. Chem. **273:**23922–23928.
48. **Weinstein, M. R., M. Litt, D. A. Kertesz, P. Wyper, D. Rose, M. Coulter, A. McGeer, R. Facklam, C. Ostach, B. M. Willey, A. Borczyk, D. E. Low, et al.** 1997. Invasive infections due to a fish pathogen, *Streptococcus iniae*. N. Engl. J. Med. **337:**589–594.
49. **Wennerstrom, D. E., J. C. Tsaihong, and J. T. Crawford.** 1985. Evaluation of the role of hemolysin and pigment in the pathogenesis of early onset group B streptococcal infection, p. 155–156. *In* Y. Kimura, S. Kotami, and Y. Shiokawa (ed.), Recent advances in streptococci and streptococcal diseases. Reedbooks, Bracknell, United Kingdom.
50. **Wertman, K. F., A. R. Wyman, and D. Botstein.** 1986. Host/vector interactions which affect the viability of recombinant phage lambda clones. Gene **49:**253–262.

Editor: E. I. Tuomanen